2023 I-RIM Conference
October 20-22, Rome, Italy
ISBN: 978-88-945805-4-9
10.5281/zenodo.10722444

Real-time lower leg muscle forces estimation using a Hill-type model and whole-body wearable sensors

Claudia Latella[1], Antonella Tatarelli[1], Lorenzo Fiori[1], Riccardo Grieco[1], Lorenzo Rapetti[1], Daniele Pucci[1,2]

I. Introduction

The estimation of the forces produced by muscles is an aspect of great interest in several fields, e.g., rehabilitation, human-machine interface and sports, where it is pivotal to estimate the muscle forces produced by the human biomechanics control system. Since muscles are the engines of human motion, the scientific community is actively involved in studying methods to model muscles in order to simulate human motions [1]. In our preliminary study, we built a computational model for the contraction dynamics estimation of three muscles of the lower leg (tibialis anterior, gastrocnemius lateralis, gastrocnemius medialis). Acquisition data have been gathered by using the iFeel technology (IMU nodes and sensorized portable shoes) developed by the Artificial and Mechanical Intelligence (AMI) of the Italian Institute of Technology (https://ifeeltech.eu) and a off-the-shelf system of surface electromyography (EMGs). The architecture has been implemented on the middleware YARP [13] for both the in-lab sensors and the EMGs tool (https://github.com/ami-iit/yarp-devices-bts-freeemg).

II. Lower leg contraction dynamics modeling

We consider three lower leg muscles: tibialis anterior, gastrocnemius lateralis and gastrocnemius medialis, Fig. 1. Muscle elements have been added into the human URDF-format model implemented in [2] usig a model-generator tool (https://github.com/ami-iit/human-model-generator) that includes skeletal and muscular properties. A contraction dynamics computational pipeline has been built for both the muscles (M) and the tendons (T), i.e., a musclulotendon (MT) complex of the lower leg and modeled by a block framework [3] [4] [5] [6] [7], Fig. 2. The pipeline runs per each muscle and each block represents a different process that actively contributes to the muscle force production, as follows.

- The **musculotendon kinematics (Block 1)** represents the kinematics of the MT complex. The block computes the length l^{MT} and the velocity v^{MT} of the complex, given lower leg joint angles s and joint velocities $\dot{s}$ readings from wearable iFeel IMU sensors.
- The **activation dynamics (Block 2)** represents the process from muscle excitation to activation [8] given the

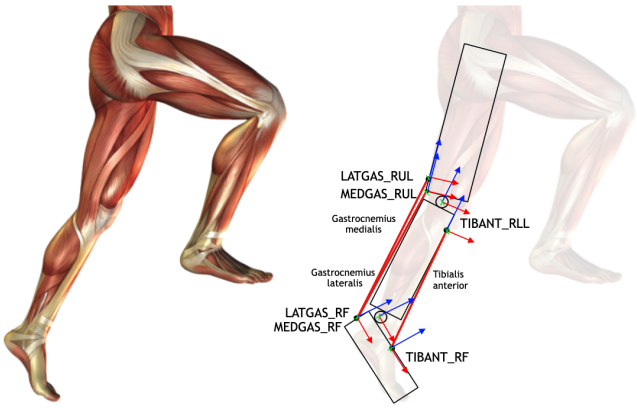

Fig. 1: Lower leg muscle modeling.

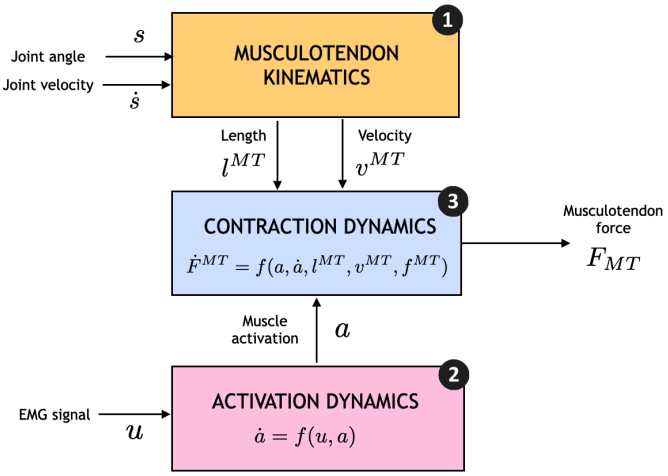

Fig. 2: Musculotendon (MT) contraction dynamics pipeline.

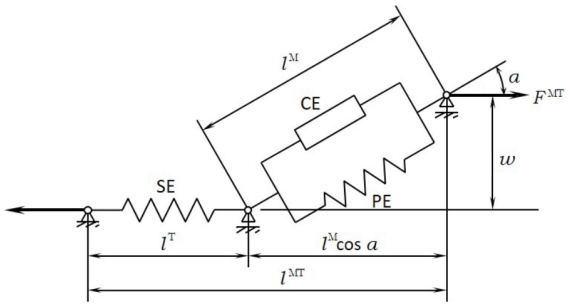

Fig. 3: Hill-type model for musculotendon complex.

[1] Artificial and Mechanical Intelligence (AMI) at Istituto Italiano di Tecnologia, Center for Robotics and Intelligent Systems, Via San Quirico 19D, Genoa, Italy. (email: name.surname@iit.it)
[2] Machine Learning and Optimisation, The University of Manchester, Manchester, United Kingdom

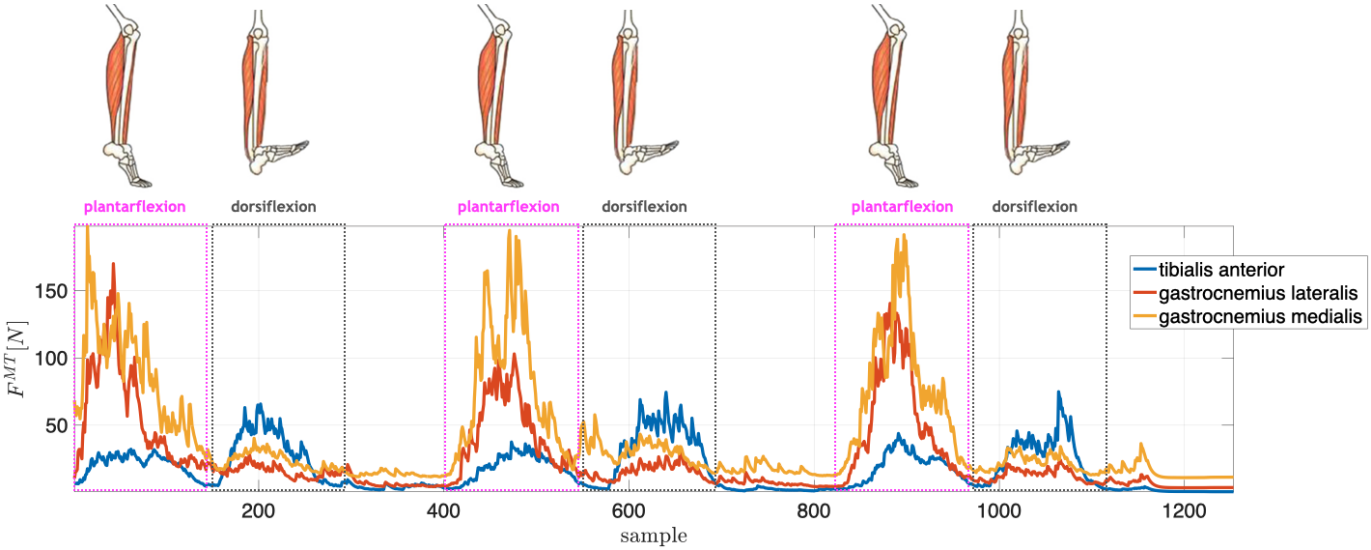

Fig. 4: Contraction dynamics estimation during three consecutive repetitions of a dorsiflexion/plantarflexion task for tibialis anterior, gastrocnemius lateralis and gastrocnemius medialis, respectively.

EMGs readings. It approximates the composite biochemical relation between muscle neuronal stimulation u and muscle activity a by a first order differential equation [9], such as

$$\dot{a} = f(u, a) = \Big((u\ c_1) + c_2\Big)(u - a)\ , \qquad (1)$$

where c_1 and c_2 are time constants taking into account the activation time τ_{ACT} for buildup of activation when the muscle is fully excited (i.e., $u = 1$) and the deactivation time τ_{DEACT} for relaxation when the muscle is deactivated (i.e., $u = 0$), i.e.,

$$c_1 = \frac{1}{\tau_{ACT}} - \frac{1}{\tau_{DEACT}}\ , \qquad c_2 = \frac{1}{\tau_{DEACT}}\ . \qquad (2)$$

- The **contraction dynamics (Block 3)** represents the process from activation to force production. The muscle dynamics is characterized by a Hill-type model, Fig. 3. It consists of three main components: i) the contractile element (CE) responsible of the active force generated by the muscle; ii) the parallel elastic element (PE) responsible for the passive elastic properties of the muscle fibers, iii) the serial elastic element (SE) representing the elasticity of the actin-miosyn crossbridges that captures the elastic properties of the tendon and the aponeurosis [10]. The overall complex force F^{MT} can be written as a composition of forces related to lenght l^{MT}, velocity v^{MT} and modulated by activation a [3] [11], such that

$$F^{MT} = \Big(a\ F_0^M F_L^{CE} F_V^{CE} + F_0^M F_L^{PE}\Big)\cos\alpha\ , \qquad (3)$$

where, F_0^M is the maximum isometric muscle force, F_L^{CE} and F_V^{CE} represent the force-length and force-velocity relationships of CE, respectively, and F_L^{PE} is the force-length relationship of PE. Angle α represents the pennation of the muscle, i.e., the angle between the direction of fibers and the direction of the line of action of the muscle (tabulated data in [12] for lower leg muscles).

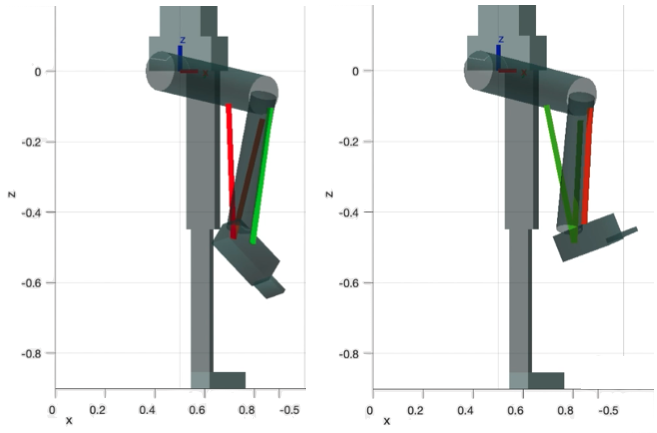

Fig. 5: Real-time visualization of lower leg muscle force estimation during a plantarflexion (*on the left*) and a dorsiflexion (*on the right*). The red colour of the line (i.e., the muscle) represents a higher level of contraction, the grreen colour a lower level of contraction.

III. Experimental Application

A healthy subject equipped with wearable distributed sensors (*iFeel IMU nodes* to detect human kinematics, a pair of *portable sensorized force/torque shoes* to detect the external forces exchanged with the ground, a wireless set of *surface electromyography probes* to detect muscle activity) performed a simple dorsiflexion/plantarflexion task. Equation 3 has been computed in real-time during the task. Figure 4 shows the estimated forces of tibialis anterior, gastrocnemius lateralis and medialis muscles during three consecutive repetitions of a dorsiflexion/plantarflexion trial. During plantarflexion, the gastrocnemii contract and their force is higher than the

tibialis force. Dorsiflexion, on the other hand, leads the tibialis anterior to contract and its force to increase more than the gastrocnemii.

A pivotal outcome of the paper is represented by the possibility to visualize in real-time the muscle forces estimation for pipeline in Fig. 2. Figure 5 shows two motion frames of a real-time visualization during the dorsiflexion/plantarflexion task. Lines attached to human links represent the muscles and their colour depends upon their activation and force production (i.e., red colour means higher contraction than green). A new YARP-based module has been added to the software architecture already presented in [14]. Overall, this boosted architecture allows for the real-time and simultaneous $i)$ readings of the sensors, $ii)$ human whole-body kinematics and dynamics estimation and $iii)$ muscle contraction dynamics estimation and visualization. Furthermore, the software tool modularity paves the way for the force estimation of *all* the muscles in the body and it is a fundamental step towards the estimation of the human whole-body joint torques.

ACKNOWLEDGMENT

The paper was supported by the Italian National Institute for Insurance against Accidents at Work (INAIL) ergoCub Project.

REFERENCES

[1] M. W. Mathis and S. Schneider, "Motor control: Neural correlates of optimal feedback control theory," *Current Biology*, vol. 31, no. 7, pp. R356–R358. [Online]. Available: https://www.sciencedirect.com/science/article/pii/S0960982221001524

[2] C. Latella, S. Traversaro, D. Ferigo, Y. Tirupachuri, L. Rapetti, F. J. Andrade Chavez, F. Nori, and D. Pucci, "Simultaneous floating-base estimation of human kinematics and joint torques," *Sensors*, vol. 19, no. 12, p. 2794. [Online]. Available: https://doi.org/10.3390/s19122794

[3] T. S. Buchanan, D. G. Lloyd, K. Manal, and T. F. Besier, "Estimation of muscle forces and joint moments using a forward-inverse dynamics model," *Medicine and Science in Sports and Exercise*, vol. 37, no. 11, pp. 1911–1916.

[4] M. Sartori, M. Reggiani, D. Farina, and D. G. Lloyd, "EMG-driven forward-dynamic estimation of muscle force and joint moment about multiple degrees of freedom in the human lower extremity," *PloS One*, vol. 7, no. 12, p. e52618.

[5] M. Millard, T. Uchida, A. Seth, and S. L. Delp, "Flexing computational muscle: modeling and simulation of musculotendon dynamics - PubMed." [Online]. Available: https://pubmed.ncbi.nlm.nih.gov/23445050/

[6] E. Ceseracciu, A. Mantoan, M. Bassa, J. C. Moreno, J. L. Pons, G. A. Prieto, A. J. d. Ama, E. Marquez-Sanchez, Gil-Agudo, C. Pizzolato, D. G. Lloyd, and M. Reggiani, "A flexible architecture to enhance wearable robots: Integration of EMG-informed models," in *2015 IEEE/RSJ International Conference on Intelligent Robots and Systems (IROS)*, pp. 4368–4374.

[7] F. Romero and F. J. Alonso, "A comparison among different hill-type contraction dynamics formulations for muscle force estimation," *Mechanical Sciences*, vol. 7, no. 1, pp. 19–29. [Online]. Available: https://ms.copernicus.org/articles/7/19/2016/ms-7-19-2016.html

[8] F. E. Zajac, "Muscle and tendon: properties, models, scaling, and application to biomechanics and motor control," *Critical Reviews in Biomedical Engineering*, vol. 17, no. 4, pp. 359–411.

[9] A. Nagano and K. G. M. Gerritsen, "Effects of neuromuscular strength training on vertical jumping performance— a computer simulation study," *Journal of Applied Biomechanics*, vol. 17, no. 2, pp. 113–128. [Online]. Available: https://journals.humankinetics.com/view/journals/jab/17/2/article-p113.xml

[10] M. S. Andersen, "Chapter 33 - rigid-body and musculoskeletal models," in *Human Orthopaedic Biomechanics*, B. Innocenti and F. Galbusera, Eds. Academic Press, pp. 659–680. [Online]. Available: https://www.sciencedirect.com/science/article/pii/B9780128244814000354

[11] H. Geyer and H. Herr, "A muscle-reflex model that encodes principles of legged mechanics produces human walking dynamics and muscle activities," *IEEE transactions on neural systems and rehabilitation engineering: a publication of the IEEE Engineering in Medicine and Biology Society*, vol. 18, no. 3, pp. 263–273.

[12] S. L. Delp, "Surgery simulation: A computer graphics system to analyze and design ... - scott lee delp - google livres." [Online]. Available: https://books.google.fr/books?id=ipzVPAAACAAJ

[13] G. Metta, P. Fitzpatrick, and L. Natale, "YARP: Yet another robot platform," *International Journal of Advanced Robotic Systems*, vol. 3, no. 1, p. 8. [Online]. Available: https://doi.org/10.5772/5761

[14] C. Latella, Y. Tirupachuri, L. Tagliapietra, L. Rapetti, B. Schirrmeister, J. Bornmann, D. Gorjan, J. Camernik, P. Maurice, L. Fritzsche, J. Gonzalez-Vargas, S. Ivaldi, J. Babic, F. Nori, and D. Pucci, "Analysis of human whole-body joint torques during overhead work with a passive exoskeleton," *IEEE Transactions on Human-Machine Systems*, pp. 1–9. [Online]. Available: https://ieeexplore.ieee.org/document/9647004/